INDIAN JOURNAL OF SCIENCE AND TECHNOLOGY

RESEARCH ARTICLE

Effect of Cryogenic Treatment on Tribological and Surface Properties of 3D Printed Thermoplastic Polyurethane

Prashant Veer[1]*, S C Vettivel[2], Jatinder Madan[2], B S Pabla[3], Leema Nelson[4]

1 Post Graduate Student, Department of Mechanical Engineering, National Institute of Technical Teachers Training and Research, 160019, Chandigarh, India
2 Department of Mechanical Engineering, Chandigarh College of Engineering and Technology (Degree Wing), Chandigarh, 160019, India
3 Department of Mechanical Engineering, National Institute of Technical Teachers Training and Research, Chandigarh, 160019, India
4 Chitkara University Research and Innovation Network (CURIN), Chitkara University Institute of Engineering & technology, Chitkara University, Punjab, India

OPEN ACCESS

Received: 12-08-2022
Accepted: 04-09-2023
Published: 27-10-2023

Citation: Veer P, Vettivel SC, Madan J, Pabla BS, Nelson L (2023) Effect of Cryogenic Treatment on Tribological and Surface Properties of 3D Printed Thermoplastic Polyurethane. Indian Journal of Science and Technology 16(40): 3491-3501. https://doi.org/10.17485/IJST/v16i40.1651

* **Corresponding author**.

prashantv.mech20@nitttrchd.ac.in

Funding: None

Competing Interests: None

Published By Indian Society for Education and Environment (iSee)

ISSN
Print: 0974-6846
Electronic: 0974-5645

Abstract

Objective: Investigating the effects of Deep Cryogenic Treatment (DCT) on the mass wear of 3D printed Thermoplastic Polyurethane (TPU) for application in knee spacers. **Methods:** Extrusion Temperature (ET), Print Speed (PS), Layer Thickness (LT), and Raster Orientation (RO), were the parameters used in this study. The mass wear of untreated and DCT TPU was obtained. The surface images were obtained through a Scanning Electron Microscope (SEM) and analyzed in the Gwyddion AFM software to investigate the surface texture, waviness, and roughness of the untreated and treated TPU. **Findings:** DCT decreased mass wear in 3D-printed TPU specimens. A higher ET (250 °C) yielded superior mass wear performance - conversely, higher PS elevated mass wear, with an optimal print speed of 15 mm/s. The most negligible mass wear was observed at 0.1 mm LT. The angle of RO exhibited significance with a 45°/135° RO orientation. Notably, PS demonstrated the most significant influence on mass wear for untreated TPU (61.11%), while for treated TPU, ET exerted the most substantial impact (90.61%). These insights were validated through analysis of variance (ANOVA) and regression modeling, indicating the robustness of the findings. **Novelty:** To date, injection-molded ultra-high molecular weight polyethylene (UHMWPE) is deployed for knee spacers. However, its rapid wear, time-consuming, and expensive fabrication techniques are a significant concern in total knee replacement surgeries. For the first time, this study combined 3D printing and deep cryogenic treatment to fabricate and characterize the tribological performance of biocompatible TPU for its potential application in knee spacers. This novel approach involved cryogenically treating the 3D-printed TPU wear specimens, which displayed superior wear performance to injection-molded UHMWPE. This affirmed the suitability of the combined 3D printing and cryogenic treatment for TPU as a potential alternative to the current methods and material for knee spacer

applications.

Keywords: 3D Printing; Deep Cryogenic Treatment; Thermoplastic Polyurethane; Mass Wear; Surface Characterization

1 Introduction

Implants' mechanical and tribological properties are pivotal in orthopedic surgery, especially in total knee replacement (TKR) procedures[1]. Mechanical properties encompass attributes like strength, elasticity, and durability, while tribological properties pertain to how materials interact under friction and wear conditions. These properties directly influence the functionality, longevity, and overall success of implanted devices such as knee spacers. Oxidation, a chemical reaction between materials and oxygen, is critical in UHMWPE implants. They can oxidize upon exposure to oxygen, forming free radicals and subsequent material degradation. This can weaken the implant's mechanical properties, induce cracks, and generate wear debris[1].

Total knee replacement (henceforth TKR) is successfully utilized to treat severely degenerated joints and is a standard procedure for treating osteoarthritic discomfort. A conventional TKR implant consists of a metallic femoral and a tibial element embedded into the femur and the tibia bone, respectively, and an insert (referred to as spacers) made of ultra-high molecular weight polyethylene (henceforth UHMWPE)[2]. Wear is a persistent problem in TKR because of its inconsistent and occasionally unstable form[2], which may eventually cause aseptic loosening, osteolysis, periprosthetic issues[3] and premature failure[2,3].

Nowadays, several biodegradable polymers have found place in biomedical applications[4,5]. UHMWPE is widely used in fabricating spacers[6]. The spacer is firmly fixed to the tibial element, and the femoral component continuously slides on it. The oxidation and wear resistance of implants and their mechanical properties are significant aspects of concern in TKR. Reducing the wear through sterilization generates free radicals, promoting oxidation in UHMWPE implants. This oxidation band on the implant's surface develops a significantly low molecular mass area, resulting in inferior mechanical properties and surface delamination. The abrasive wear caused by the sliding motion of the femoral element on the spacer's surface generates wear debris, causing cytokine response and osteolysis[6]. Such implant deteriorating events quicken the need for an inevitable second surgery.

The UHMWPE spacers are traditionally made using injection molding or freeze-casting processes. The fundamental drawback of these techniques is the inability to manage the micro and macro-pore sizes[7]. The implant's surface geometry impacts the knee joint's conformance and engagement biomechanics. The patient's knee proportions vary with gender, age, and disease. With this variation, molds and cavities specific to the joint conditions need to be prepared. There is no standardized size for the implants. Thus, for every patient, this process has to be repeated, which makes it time-consuming and cost-ineffective. Other limitations in traditional methods include limited control over surface roughness and elasticity[7].

Thermoplastic polyurethane (henceforth TPU), which has excellent physical and mechanical properties and is biocompatible[8,9], is employed in the medical field[10]. A superior combination of flexibility and mechanical performance of TPU is attributable to its structure of soft segments (offering the flexible nature to TPU) and hard segments (providing strength)[11].

The usage of 3D printing technologies in patient-specific therapies has expanded manifold. Implants customized per the patient's requirements can be made using 3D printing. From a CT scan to 3D printing, a personalized knee replacement can speed up healing, fabrication, and operation speed and guarantee proper alignment[7]. The approach has demonstrated its value by reducing costs, increasing mechanical

properties, and optimizing time consumption. The most significant use of 3D printing in orthopedics is creating scaffolds with complete control over pore size, shape, and properties [7].

Deep cryogenic treatment (henceforth DCT) is used to improve materials' mechanical and tribological characteristics. Subjecting materials to a sub-zero temperature of around -196°C refines the microstructure [12]. Even after bringing the sample back to ambient temperature, the properties obtained after DCT are preserved [12]. A vast amount of literature review on the subject has stressed that the DCT of polymers causes significant changes in their mechanical characteristics [13]. The properties of machining tools and carbon-fiber polyimide [13] PEEK (poly-ether ether ketone), ABS (acrylonitrile butadiene styrene), PA6 (polyamide), and PI (polyimide) [14] enhance with DCT. Injection-molded UHMWPE, when subjected to DCT, generated local thermally sensitive excitations and organized disturbance of the crystalline ordering of chains, degrading its structure [14]. The above discussion summarizes the significant issues in developing biomedical implants in Table 1 (a).

While publications on 3D printed UHMWPE, 3D printed TPU, and the DCT of UHMWPE and TPU fabricated by methods other than 3D printing are separately available, limited work has been discovered that combines DCT technique and 3D printing of components, with TPU as a potential alternative to UHMWPE for spacers [9]. Further, a comparative analysis of the effect of DCT on tribological and surface characteristics of FDM fabricated TPU is not yet reported.

Introducing the powerful synergy between 3D printing and deep cryogenic treatment (DCT), this study strategically combines these techniques to address the shortcomings inherent in traditional fabrication methods for knee spacers. By harnessing the precision of 3D printing technology and the structural enhancements conferred by DCT, this innovative approach aims to overcome the limitations of conventional techniques, such as injection molding, which need help with customized sizing, surface roughness control, and mechanical performance. This novel integration holds the potential to significantly enhance knee spacer performance by offering tailored designs, improved material properties, and enhanced wear resistance, ultimately paving the way for more successful and enduring total knee replacement surgeries. Hence, this study aims to examine the

- Influence of DCT on the tribological performance of FDM fabricated TPU.
- Influence of FDM printing parameters on the tribological performance of FDM fabricated TPU.
- Impact of DCT on topographical properties like roughness, texture, waviness, skewness, and kurtosis of FDM fabricated TPU.

The purpose of the present work is to investigate the suitability of TPU and FDM as the potential material and fabrication methods, respectively, for knee spacers instead of UHMWPE and injection molding, as well as to use DCT to improve the wear performance of FDM fabricated TPU. The presently used approach and the proposed approach used for this study are depicted in Table 1 (b).

Table 1. (a) Major issues in developing knee spacers with currently used materials and techniques; (b) the current and the proposed materials and techniques for knee spacers

(a) Major issues in developing knee spacers with current materials and techniques		
Category	Currently used material/ technique	Major issues
Materials	UHMWPE	Oxidation leads to osteolysis and cytokine response.
Fabrication technique	Injection molding	• Inflexibility to customize implants as per the patient's requirements. • Limited control over pore size and surface quality. • Higher fabrication cost (due to the requirement of different molds for making patient-specific implants. • Time-consuming
Tribological performance		Continuous wear of spacer by the femoral element.
(b) The current and the proposed materials and techniques for knee spacers		
Category	Currently used material/ technique	Proposed material/ technique
Material	UHMWPE	TPU
Fabrication technique	Injection molding	3D printing (FDM)
Method to improve the wear performance	–	DCT

3D printing is a promising field that offers flexibility in mass customization and development of end-user functional parts. DCT has proven its superior capability to improve polymers' mechanical and tribological performance. The proposed novel approach aims to solve the critical issue of providing flexibility in the customization of knee spacers (through 3D printing) and reducing wear (by subjecting them to DCT), thus enhancing the life of knee spacers.

2 Methodology

2.1 Specimen Preparation

This experiment examined a commonly available TPU filament of 1.75 mm diameter manufactured by SolidSpace Technologies (Maharashtra, India). According to the supplier, its properties are summarized in Table 2 (a). The 12 mm cross-section and 30 mm thickness wear test specimens were printed per ASTM G99 standards. The design was prepared in Creo Parametric (version 6.0) software. Four printing parameters, namely extrusion temperature (ET), print speed (PS), layer thickness (LT), and raster orientation (RO), were chosen for investigation. The combinations of these parameters were obtained from the Taguchi method of robust design of experiments. Twenty-seven experimental runs (L27) of various parametric combinations were undertaken. The infill pattern chosen was the solid (line) structure for printing, while the infill density was kept at 100 %. The bed temperature was kept fixed at 50 °C.

Three levels were selected in this study, as displayed in Table 2 (b).

Table 2. (a) Filament properties; (b) Process Parameters

(a) Filament properties			
Physical properties	Test method	Units	Value
Hardness	ISO 868	Shore D	53
Specific gravity	ISO 2781	g/cm3	1.15
Modulus of elasticity	ISO 527	MPa	78
Tensile strength at break	ISO 527	Mpa	52
Elongation at break		%	525
(b) Process Parameters			
Parameter	Abbreviation	Units	Levels
Extrusion temperature	ET	°C	220, 235, 250
Print speed	PS	mm s^{-1}	15, 37.5, 60
Layer thickness	LT	mm	0.1, 0.2, 0.3
Raster orientation	RO	°	0, 45/135, 90

Diagrammatic representation of the design and the printed specimens is shown in Figure 1.

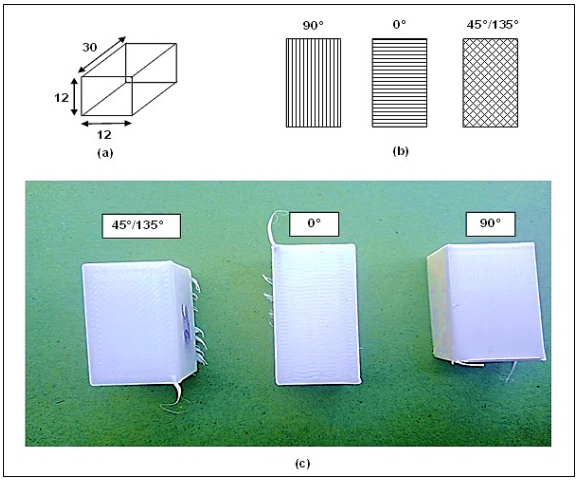

Fig 1. Diagrammatic representation of (a) dimensions of the wear specimen, (b) different raster orientations, (c) 3D printed specimens

FDM fabricated wear specimens were exposed to controlled DCT in the cryogenic processing chamber (Cryo processor, Primero Enserve, Chennai) available at the Institute of Auto Parts and Hand Tools Technology, Ludhiana. The temperature of 77 K was attained at a rate of 0.52 °C min^{-1}, and the specimens were soaked for 24 hours. They were brought back to normal temperature at the same rate as before. To protect specimens' sharp or sensitive edges, they were wrapped in a thin aluminum foil before placing them in the chamber.

2.2 Characterization

2.2.1 Tribological Characterization

Before conducting any wear analysis, the wear specimens were weighed using an anti-electrostatic digital weighing machine with an accuracy of 0.0001 g (Vibra HT weighing machine, Japan). The printed samples were tested on a Ducom Tribometers dry wear rig (Ducom Tribometers Inc.) for 30 minutes with a constant applied load of 80 N[14]. A track diameter of 100 mm and 100 rpm speed were taken for the study[14]. After the wear, the samples were cleaned for debris and weighed again. The final mass obtained after the wear test was subtracted from the initial measurements, thus providing the mass wear loss. The mass wear was obtained by equation (a).

$$\text{Mass wear}(\%) = 100 * [\text{ Initial mass of the specimen } - \text{ Final mass of the specimen }] / \text{ Initial mass of the specimen} \quad \text{(a)}$$

2.2.2 Surface Characterization

The worn-out surfaces of the wear samples were examined using a scanning electron microscope (henceforth SEM) (JEOL 6380A) to investigate the wear mechanism involved in untreated and cryogenically treated TPU. The images were recorded at 100 μm, 200 μm, and 500 μm. The SEM images were then uploaded to Gwyddion software (version 2.6). It is an Atomic Force Microscopy (AFM) software capable of generating 3D profiles of the surfaces from 2D SEM images. The texture, waviness, roughness plots, and other surface properties, such as skewness and Kurtosis, were also analyzed.

3 Results and Discussion

"The lower, the better" approach analyzed the mass wear responses for untreated and treated TPU. Figure 2 (a) shows that the optimum parameters for mass wear of untreated TPU were 250 °C ET, 15 mm/s PS, 0.3 mm LT, and 90° RO. The parameter combinations in the order of decreasing significance for untreated TPU were PS- LT- ET- RO. For treated TPU, the optimum values of parameters were 250 °C ET, 15 mm/s PS, 0.3 mm LT, and 45°/135° RO (Figure 2 (b)). The order of parameters for treated TPU in terms of significance was ET- PS- RO- LT (Table 3 (a)).

Table 3 (b) shows the % contribution of each parameter and their effect on the untreated and treated specimens' mass wear. The PS had the maximum influence on the mass wear of untreated TPU (61.11%), followed by LT (15.96%), ET (15.93%), and RO (6.99%). However, the treated TPU depicted a different behavior. The ET majorly influenced the mass wear of treated TPU (90.61%), followed by PS (7.52%), RO (1.57%), and lastly, LT (0.29%). According to the ANOVA, PS had a substantial impact on untreated TPU's mass wear, and for treated TPU, ET had a significant effect on mass wear. The linear regression analysis showed that there was no transformation in each response. Table 3 (c) contains the empirical relationship between the process parameters and the R^2 value for untreated and treated specimens. The generated regression models for untreated and treated TPU's mass wear in the current study had high R^2 values of 90.93% and 83.78%, respectively.

Table 3 (d) includes the ANOVA analyses for the untreated and treated TPU mass wear.

Figure 2 (c) and (d) display the Pareto charts of the standardized effects and the normal probability plots for untreated and treated TPU, respectively.

The importance of the coefficients in the projected model was examined using the residual plot. The residual plot is linear, and the residual errors are distributed normally; thus, the model's coefficients are essential. Both untreated and treated TPU's mass wear residuals are close to the straight line, suggesting that the established models are substantial.

Figure 3 contains the contour plots for untreated and treated TPU mass wear. Figure 3 (a-b) shows lower mass wear is obtained at high ET and low PS for untreated and treated TPU. A high LT and high ET for untreated gave lower mass wear (Figure 3 (c)), but for the treated TPU, the LT effect was insignificant (Figure 3 (d)). Figure 3 (e-f) shows that higher ET and 90° RO for untreated and treated TPU offered lower mass wear. Figure 3 (g-h) shows lower PS and higher LT for untreated and treated TPU delivered lower mass wear. Lower PS and 90° RO for untreated and treated TPU offered lower mass wear (Figure 3 (i-j)). However, the effect of LT was not that significant in treated TPU's mass wear. Figure 3 (k-l) shows higher LT and 90° RO for untreated, offering the best mass wear.

Table 3. (a) SN ratio response table for untreated and treated specimens; (b) % Contribution of process parameters on untreated and treated specimen mass wear; (c) Empirical relationship and R^2 value for untreated and treated TPU; (d) ANOVA analyses for untreated and treated TPU mass wear

(a) SN ratio response table for untreated and treated specimens

	Untreated TPU				**Treated TPU**			
Level	ET	PS	LT	RO	ET	PS	LT	RO
1	-69.33	-68.99	-69.37	-69.27	-69.98	-67.25	-67.22	-68.01
2	-69.27	-69.13	-69.22	-69.28	-68.66	-67.61	-67.84	-67.54
3	-69.05	-69.54	-69.07	-69.11	-65.54	-68.33	-67.63	-67.64
Delta	0.28	0.56	0.29	0.18	3.43	1.07	0.22	0.47
Rank	3	1	2	4	1	2	4	3

(b) % Contribution of process parameters on untreated and treated specimen mass wear

	Untreated TPU				**Treated TPU**			
Source	SS	MS	% Contribution	Influence rank	SS	MS	% Contribution	Influence rank
ET	0.130112	0.065056	15.93	3	21.622	10.811	90.61	1
PS	0.499014	0.249507	61.11	1	1.7949	0.8975	7.52	2
LT	0.130352	0.065176	15.96	2	0.0703	0.0352	0.29	4
RO	0.057164	0.028582	6.99	4	0.3745	0.1872	1.57	3
Total	0.816642		~100		23.862		~100	

(c) Empirical relationship and R^2 value for untreated and treated TPU

	Untreated TPU	**Treated TPU**
Empirical relationship	3577 – 3.04 ET + 4.126 PS – 494 LT – 0.590 RO	9434 – 30.41 ET + 6.32 PS – 40 LT – 0.88 RO
R^2	90.93%	83.78%

(d) ANOVA analyses for untreated and treated TPU mass wear

	Untreated TPU		**Treated TPU**	
Source	p-value	Significance ($p < 0.05$)	p-value	Significance ($p < 0.05$)
Regression	0.023	Significant	0.070	Insignificant
ET	0.070	Insignificant	0.012	Significant
PS	0.009	Significant	0.249	Insignificant
LT	0.056	Insignificant	0.972	Insignificant
RO	0.226	Insignificant	0.727	Insignificant

The parameter-wise variation of mass wear for untreated and treated TPU is discussed in this section. Figure 4 (a) shows that the increase in ET decreased mass wear for both untreated and treated specimens. Thus, a higher ET offered better mass wear for untreated and treated samples. The optimum ET was 250 °C. This behavior can be attributed to improved material flow and interlayer adhesion, resulting in a more cohesive structure with lower susceptibility to wear.

Figure 4 (b) depicts the variation of mass wear with print speed (PS). The mass wear for both untreated and treated TPU increased with PS. This behavior vouched for the fact that higher PS had a detrimental effect on the coefficient of friction. This outcome aligns with the principle that excessive PS can lead to inadequate material bonding and increased wear rates. For both untreated and treated specimens, the most suitable PS was 15 mm/s. A higher LT deteriorated the mass wear of untreated TPU. Still, this variation is not that significant, while for treated TPU, the mass wear for 0.1 mm and 0.2 mm LT were almost the same, but it was slightly lower at 0.3 mm. The optimum wear performance was obtained at an LT of 0.1 mm. Thus, for both untreated and treated TPU, lower LT positively affected the mass wear (Figure 4 (c)). The same was confirmed by [7]. The lowest mass wear for untreated and treated TPU was reported at 45°/135, as shown in Figure 4 (d).

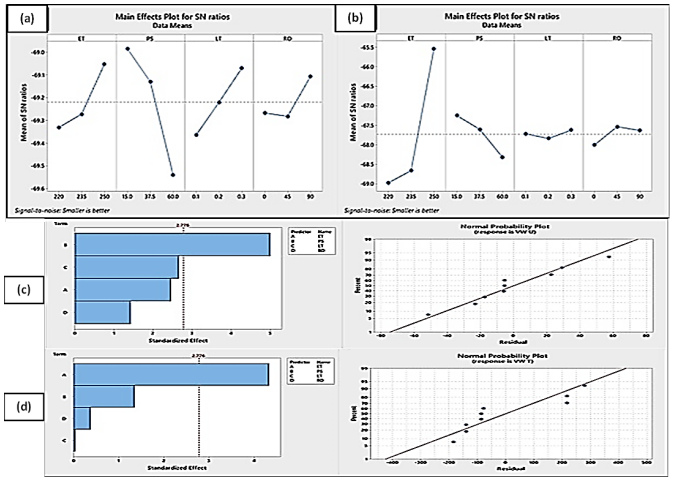

Fig 2. Mean SN ratio plots of (a) untreated TPU mass wear; (b) treated TPU mass wear and Pareto charts of the standardized effects (left) and the normal probability plots (right) for (a) untreated TPU; (b) treated TPU

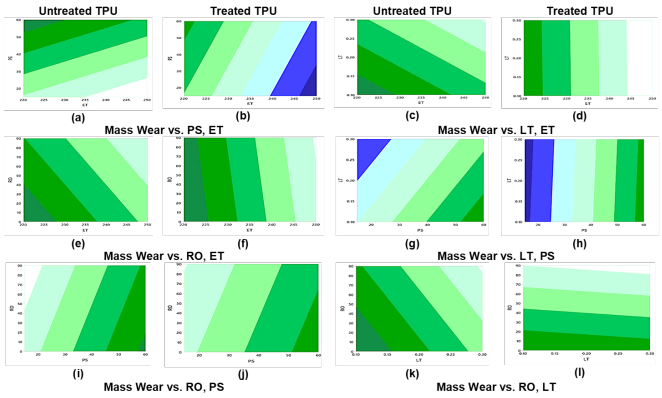

Fig 3. Contour plots for untreated and treated TPU mass wear

Table 4 enlists the materials, the fabrication techniques, the deployed methodologies for the wear test, and the serial number in which their respective results are depicted in Figure 4 (e).

The following discussion focuses on investigating and highlighting the suitability of FDM compared to other fabrication techniques for knee spacers. The egg albumen has been deployed by[14] which mimics the synovial fluid in the knee joint. The wear rates of these lubrication wear have been specially incorporated to compare them with our study that involves untreated and treated TPU. This has been done purposely to see whether the untreated and the DCT TPU prepared by FDM can offer similar or superior results as compared to injection molded UHMWPE, subject to lubricated wear, which is an imitation of the injection molded UHMWPE spacer inside the body, surrounded with body fluids and bearing the wear load from the femoral element. (i) represents the wear rate of MJF fabricated TPU. Its wear has been recorded as the highest among all other wear rates, rendering MJF ineffective for fabricating knee spacers.

Comparable results to (i) can be seen in (iv) and (vi), which correspond to dry wear of injection molded UHMWPE treated for 24 hours and 12 hours, respectively. From (ii) and (vii), it is evident that the lubrication wear offered lesser wear rates than dry wear conditions. (viii) offered the same wear as UHMWPE treated for 12 hours and worn in lubricated conditions. This suggests that FDM fabricated TPU when worn without lubrication, can offer the same results as the treated UHMWPE worn in lubricated conditions. Further, an even lower wear rate was obtained in (ix). This affirms that FDM and TPU are suitable alternatives to the current methods and materials for fabricating knee spacers, i.e., injection molding and UHMWPE. From Figure 4 (e), it is clear that the order of decreasing wear rates is as follows: TPU by MJF, dry wear> DCT injection molded UHMWPE> untreated FDM fabricated TPU> DCT FDM fabricated TPU> untreated injection molded UHMWPE.

Table 4. (a) Materials, fabrication techniques, and the deployed methodologies for the wear test in various studies; (b) Color coding of results and their corresponding order in Figure 4 (e)

(a) Materials, fabrication techniques, and the deployed methodologies for the wear test in various studies

	Material	Fabrication technique	Deployed methodologies for the wear test
(7)	TPU	Multi Jet Fusion (MJF)	Before the test, the specimens were ground and polished to provide a flatter surface. A Si3N4 ball with a radius of 3.175 mm was then placed against each specimen at a normal load of 35 N after each specimen had been firmly fastened in the sample holder. For 45 minutes, the ball reciprocated linearly with a 10 mm stroke length at 10 mm/s.
(11)	UHMWPE	Injection molding	Over 30 minutes, the specimen pin was continuously abraded against the steel disc. The same was chosen with the following parameters: 100 RPM speed, 120 mm track diameter, and 80 N load. Egg albumen has been utilized as a lubricant for lubrication wear because it is biocompatible and has a viscosity comparable to the synovial fluid found in the body.
The present study	Untreated and deep cryogenically treated (DCT) TPU	FDM	The samples were abraded for 30 minutes (11) against the steel disc at 100 RPM speed, 100 mm track diameter, and 80 N load.

(b) Colour coding of results and their corresponding order in Figure 4 (e)

	Color coding in Figure 4 (e)	Order in Figure 4 (e)
(7)	Red	(i)
(11)	Yellow	(ii – vii) (ii): untreated UHMWPE, dry wear, (iii): untreated UHMWPE, lubricated wear, (iv): UHMWPE treated for 24 hours, dry wear, (v): UHMWPE treated for 24 hours, lubricated wear, (vi): UHMWPE treated for 12 hours, dry wear, (vii): UHMWPE treated for 12 hours, lubricated wear
The present study	Green	(viii): FDM printed untreated TPU (present study) (ix) FDM printed deep cryogenically treated TPU (present study)

Figure 4 (f) shows comparative images of worn untreated and treated TPU. Compared to the rugged topography in treated TPU surfaces, the surface texture of untreated TPU looked relatively smooth. In treated TPU, delamination has occurred on the surface. The cracks are perpendicular to the direction of wear.

It is evident from Figure 4 that a higher ET, lower PS, lower LT, and 45°/135° offered lower mass wear. This behavior is attributable to higher ET offering higher flowability and better material extrusion from the nozzle (12). Lower PS ensured the smooth flow of the material by avoiding any turbulence during extrusion. Combining these two parameter settings helped reduce the voids between layers, thus achieving enhanced inter-layer adhesion and superior bonding between layers (15,16). At lower LT, as the heated nozzle is relatively closer to the bed, it acts as an additional heat source for the layer printed on the previous layer (15,17,18). This ensures proper adhesion of layers. 45°/135° RO offers cross-directional laying of layers, providing better strength to the specimens. This enhanced strength is also due to the reduced pores in 45°/135° RO compared to unidirectional layups. The increased ruggedness of treated TPU, as shown in Figure 4 (f), can be attributed to the surface contracting under a cryogenic environment and then expanding unevenly when brought to room temperature. These topographical changes could have been caused by residual stresses in the polymer caused by temperature differences and residual strains caused by the contractive forces.

The SEM images of both untreated and treated TPU were analyzed for their surface properties in the Gwyddion software. The interpolation type used was linear to generate the 3D profiles from the SEM images. A mean line is drawn at the center of the SEM image. All the values are calculated over the length of this line. Table 5 includes the surface properties of untreated and treated TPU obtained by the Gwyddion software.

Table 5 shows that the surface roughness of untreated TPU is less than that of treated TPU. The Amplitude Distribution Function (ADF) measures the probability of the profile's height at any point on the mean line. Skewness defines the shape of ADF. It is a measure of the symmetry of the profile variation about the mean line. From Table 5, it is evident that the profile

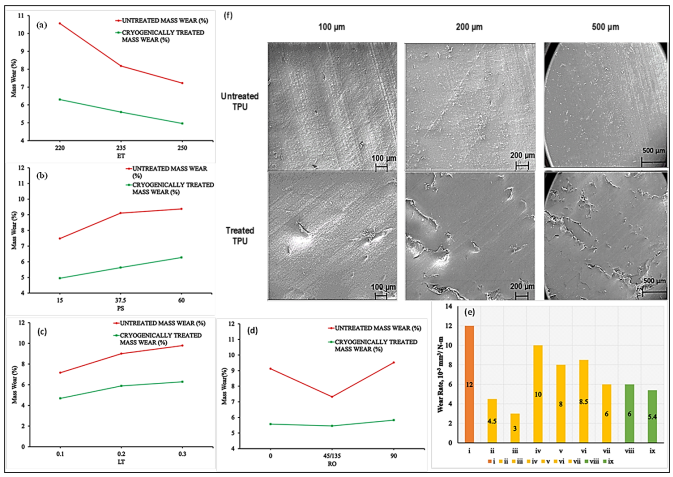

Fig 4. (a) Variation of mass wear (%) of untreated and DCT TPU with ET; (b) Variation of mass wear (%) of untreated and DCT TPU with PS; (c) Variation of mass wear (%) of untreated and DCT TPU with LT; (d) Variation of mass wear (%)of untreated and DCT TPU with RO; (e) Variation of wear rate of (i) TPU fabricated by MJF, (ii) untreated UHMWPE fabricated by injection molding (drywear), (iii) untreated UHMWPE fabricated by injection molding (lubricated wear), (iv) Injection molded UHMWPE treated for 24 hours (dry wear), (v) Injection molded UHMWPE treated for 24 hours (lubricated wear), (vi) Injection molded UHMWPE treated for 12 hours (dry wear), (vii) Injection molded UHMWPE treated for 12 hours (lubricated wear), (viii) FDM printed untreated TPU (present study), (ix) FDM printed deep cryogenically treated TPU (present study); (f) SEM images of worn TPU wear specimens at 100 μm, 200 μm, and 500 μm

Table 5. Surface properties of untreated TPU and treated TPU worn surface

Abbreviation	Property	Untreated TPU	Treated TPU
R_a	Average roughness	61.99 nm	81.95 nm
R_q	Root means square roughness	90.02 nm	103.1 nm
R_t	Maximum height of the roughness	900.8 nm	715.0 nm
R_v	Maximum roughness valley depth	386.1 nm	310.4 nm
R_p	Maximum roughness peak height	514.7 nm	404.6 nm
R_{sk}	Skewness	0.1617	0.2716
R_{ku}	Kurtosis	3.637	6.036
W_a	Waviness average	137.2 nm	67.18 nm
W_q	Root means square waviness	189.0 nm	81.20 nm

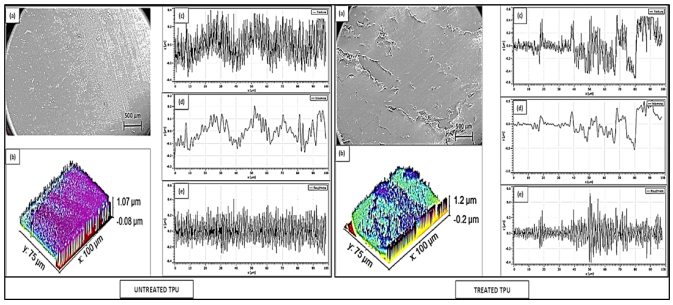

Fig 5. Images of (a) SEM profile at 500 μm, (b) 3D profile generated from theSEM image, (c) surface texture plot, (d) surface waviness plot, (e) surfaceroughness plot of untreated and treated TPU

of treated TPU is more asymmetrical than untreated TPU. A higher kurtosis of treated TPU suggests its profile is spikier than untreated TPU. This suggests a negative influence of DCT on the surface roughness of TPU specimens. These attributes are visible in Figure 5.

4 Conclusion

The present study establishes a novel combination of fused deposition modeling (FDM) and deep cryogenic treatment (DCT) as a superior potential alternative to the current methods and materials for fabricating knee spacers for TKR surgeries. The outcomes of this study offer insight into the fundamental characteristics unique to the FDM process and DCT. They can be deployed as a standard for comparative analysis with different materials fabricated through other techniques. Further, the optimized combination of FDM process parameters has been obtained that affirmed improved tribological and surface characteristics. The following conclusions are obtained from this study:

- The mass wear of deep cryogenically treated TPU was lower than that of untreated TPU. This indicated that DCT can effectively improve the wear performance of materials used in knee spacers.
- The mass wear has predicted efficiencies with 90.93% confidence for untreated TPU and 83.78% for treated TPU. Both untreated and treated TPUs wear residuals are close to the straight line, suggesting that the established models are substantial.
- The mass wear decreased with an increase in ET. Higher PS and LT deteriorated the wear performance. The lowest wear was observed for 45°/135° RO.
- The surface of treated TPU was rougher than that of untreated TPU. Higher waviness and spikier surfaces were obtained in treated TPU. Such behavior is attributable to contraction under a cryogenic environment and uneven expansion while bringing to ambient conditions.

More effort is required to develop a clear indication of the underlying theories and mechanisms related to FDM printing and cryogenic treatment, which will aid in addressing challenges such as inferior surface finish and dimensional accuracy and the cost of the setup so that this revolutionary combination of technologies attains the potential to be deployed on a bigger scale.

References

1) Veer P, Pabla BS, Madan J, Chidambaranathan VS. Fused deposition modeling in knee arthroplasty: review with the current and novel materials. In: K KR, C VS, R S, editors. Mechanical Properties and Characterization of Additively Manufactured Materials;vol. 2023. CRC Press. 2023;p. 211–235. Available from: https://doi.org/10.18063/ijb.v8i4.615.
2) Zhang M, Wang JYY, Su J, Wang JJY, Yan STT, Luan YCC, et al. Wear Assessment of Tibial Inserts Made of Highly Cross-Linked Polyethylene Supplemented with Dodecyl Gallate in the Total Knee Arthroplasty. *Polymers*. 2021;13(11):1847. Available from: https://doi.org/10.3390/polym13111847.
3) Gemayel AC, Matthew V. Total Knee Replacement Techniques. . Available from: https://www.ncbi.nlm.nih.gov/books/NBK538208/.
4) Kumar A, Behl T, Chadha S. Synthesis of physically crosslinked PVA/Chitosan loaded silver nanoparticles hydrogels with tunable mechanical properties and antibacterial effects. *International Journal of Biological Macromolecules*. 2020;149:1262–1274. Available from: https://doi.org/10.1016/j.ijbiomac.2020.02.048.
5) Thakur G, Singh A, Singh I. Chitosan-Montmorillonite Polymer Composites: Formulation and Evaluation of Sustained Release Tablets of Aceclofenac. *Scientia Pharmaceutica*. 2015;84(4):603–617. Available from: https://doi.org/10.3390/scipharm84040603.
6) Bistolfi A, Giustra F, Bosco F, Sabatini L, Aprato A, Bracco P, et al. Ultra-high molecular weight polyethylene (UHMWPE) for hip and knee arthroplasty: The present and the future. *Journal of Orthopaedics*. 2021;25:98–106. Available from: https://doi.org/10.1016/j.jor.2021.04.004.
7) Rouf S, Haq RAIU, Naveed M, Jeganmohan N, S. Farzana Kichloo A. 3D printed parts and mechanical properties: Influencing parameters, sustainability aspects, global market scenario, challenges and applications. 2022. Available from: https://doi.org/10.1016/j.aiepr.2022.02.001.
8) Chen D, Li J, Yuan Y, Gao C, Cui Y, Li S. A Review of the Polymer for Cryogenic Application: Methods, Mechanisms and Perspectives. 2021. Available from: https://doi.org/10.3390/polym1303.
9) Veer P, Vettivel SC, Madan J, Pabla BS. Biocompatibility characterization of cryogenically treated FDM printed thermoplastic polyurethane. *Materials Today: Proceedings*. 2023. Available from: https://doi.org/10.1016/j.matpr.2023.09.049.
10) Mrówka M, Szymiczek M, Machoczek T, Pawlyta M. Influence of the Halloysite Nanotube (HNT) Addition on Selected Mechanical and Biological Properties of Thermoplastic Polyurethane. *Materials*. 2021;14(13):3625. Available from: https://doi.org/10.3390/ma14133625.
11) Tey WS, Cai C, Zhou K. A Comprehensive Investigation on 3D Printing of Polyamide 11 and Thermoplastic Polyurethane via Multi Jet Fusion. *Polymers*. 2021;13(13):2139. Available from: https://doi.org/10.3390/polym13132139.
12) Singh G, Pandey KN. Effect of cryogenic treatment on properties of materials: A review. *Proceedings of the Institution of Mechanical Engineers, Part E: Journal of Process Mechanical Engineering*. 2022;236(4):1758–1773. Available from: https://doi.org/10.1177/09544089221090189.
13) Vinod B, Sudev LJ. Effect of cryogenic treatment on mechanical behavior of PALF reinforced polymer composite. *Materials Today: Proceedings*. 2022;64:330–337. Available from: https://doi.org/10.1016/j.matpr.2022.04.692.
14) Chopra S, Deshmukh KA, Somvanshi MV, Patil NV, Rakhe SR, Sontakke RV, et al. Structural Elucidation and Mechanical Behavior of Cryogenically Treated Ultra-High Molecular Weight Poly-ethylene (UHMWPE). *Transactions of the Indian Institute of Metals*. 2021;74(2):255–265. Available from: https://doi.org/10.1007/s12666-020-02140-2.

15) Kasmi S, Ginoux G, Labbé E, Alix S. Multi-physics properties of thermoplastic polyurethane at various fused filament fabrication parameters. *Rapid Prototyping Journal*. 2022;28(5):895–906. Available from: https://doi.org/10.1108/RPJ-08-2021-0214.
16) Ginoux G, Vroman I, Alix S. Influence of fused filament fabrication parameters on tensile properties of polylactide/layered silicate nanocomposite using response surface methodology. *Journal of Applied Polymer Science*. 2021;138(14). Available from: https://doi.org/10.1002/app.50174.
17) Magri AE, Mabrouk KE, Vaudreuil S, Chibane H, Touhami ME. Optimization of printing parameters for improvement of mechanical and thermal performances of 3D printed poly(ether ether ketone) parts. *Journal of Applied Polymer Science*. 2020;137(37). Available from: https://doi.org/10.1002/app.49087.
18) Podsiadły B, Skalski A, Rozpiórski W, Słoma M. Are We Able to Print Components as Strong as Injection Molded?—Comparing the Properties of 3D Printed and Injection Molded Components Made from ABS Thermoplastic. *Applied Sciences*. 2021;11(15):6946. Available from: https://doi.org/10.3390/app11156946.